Rotman Lens Amplitude, Phase, and Pattern Evaluations by Measurements and Full Wave Simulations

Junwei Dong [1], Amir I. Zaghloul [1, 3], Rensheng Sun [2], C. J. Reddy [2], Steven J. Weiss[3]
[1] Department of Electrical & Computer Engineering
Virginia Polytechnic Institute and State University, VA 22043, USA
djwei@vt.edu , amirz@vt.edu

[2] EM Software & Systems (USA)
144 Research Dr, Hampton, VA 23666, USA
ray@emssusa.com, cjreddy@emssusa.com

[3] U.S. Army Research Laboratory, Adelphi, MD 20783, USA
amir.zaghloul@us.army.mil , steven.weiss@us.army.mil

Abstract ─ Microwave lens' performance is depicted by several parameters such as phase error, amplitude taper, and array scan pattern etc. For decades, these parameters have been estimated by the geometry optics method that does not capture the mutual couplings within the lens geometry. Full wave simulation toolkits to conduct EM prediction are now available. However, using them to synthesize and optimize the electrical performance of Rotman lens is still relatively new. Several microwave lens full wave simulations have been attempted using different methods, such as FDTD, FEM, and FIT. They were reported from the perspectives of either phase or amplitude predictions at a single port or single frequency. However, the lens properties at multiple frequencies and for multiple beam ports using MoM have not been investigated. In this paper, we address such simulations using the planar Green's function in FEKO. The phase, amplitude and array factor across the frequency band for multiple beam ports are compared with the measured results, and their errors are evaluated. Prominent agreement between FEKO and measurement is demonstrated. The performance of a prototype lens is presented, followed by discussing few future aspects of lens optimization using full wave simulations.

Index Terms ─ Microstrip Lens, Rotman Lens, MoM, FEKO, Mutual Coupling.

I. INTRODUCTION

In radar and communications array systems, the Beam Forming Network (BFN) is a critical device that produces feeding phases and amplitudes for the antenna elements to perform electrical scanning. Two popular passive BFNs are the Butler Matrix and Bootlace/Rotman lens [1]. The Rotman Lens has superior performance to the Butler Matrix because of its intrinsic True Time Delay (TTD), wide band and wide scan angle characteristics. To design a microwave lens, one follows geometrical optics models [1, 2, 3] to formulate initial phase centers of the input and output ports. Then physical implementations are applied by using waveguide, stripline or microstrip mechanisms. The mutual couplings between the adjacent ports as well as the multiple reflections are not predicted using the initial direct ray formulation. Consequently, to draw reasonable predictions of the phase and amplitude information, accurate analysis tools such as full wave solvers are desired. In recent years, researchers have analyzed Rotman Lens using different numerical techniques, including with finite different time domain (FDTD) in XFDTD [4], with finite element method (FEM) in HFSS [5], and with finite integration technique (FIT) in CST Microwave Studio [6]. However, to conduct lens optimization, more efficient and accurate methods are still in demand. In this paper, we analyze one printed microstrip lens. Given the nature of the printed structure of this lens, method

of moments (MoM) with planar Green's Function is very suitable in terms of both accuracy and computation efficiency.

The Rotman Lens under consideration is 8x8 microstrip lens (8 scanning beams, 8 fed array elements). To capture its general performance, we evaluate the phase and amplitude coupling between each beam port and receiving port across the frequency band, as well as the single port to aperture phase and amplitude couplings. Pattern performance is achieved by calculating the array factor using the simulated and measured amplitude and phase information. The errors occurred in the phases, amplitudes and radiation pattern are emphasized through post processing by assuming a linear phase shift, uniform amplitude distribution and true time delay design. Simulation results are compared with the measurement across the frequency band of 4-5 GHz throughout the evaluation.

II. ROTMAN LENS MODEL

Electrically steerable array system uses Beam Forming Networks (BFN) to form different phase fronts across the aperture for different input excitations. In doing so, it achieves planar waves traveled to separate spatial directions by simply switching the inputs, as shown in Fig. 1(a). Microwave lens, connecting each input to a beam port, utilizes a lens cavity and transmission lines to guide the wave propagation. By properly controlling the beam port positions, receiving port positions and transmission line lengths, the lens is able to achieve the linear phase front across the array output, as indicated in Fig. 1(b). These parameters can be determined by theories of the traditional trifocal lens [1], the quadrufocal lens [2], or the non-focal lens [3]. Upon achieving this information, the port and cavity can be implemented in waveguide, microstrip or stripline media, while the transmission lines can be realized by either the same medium or separate cables.

The Rotman lens presented in this paper is built on the microstrip laminate Rogers 5870. Lens layout is shown in Fig. 2, whose beam ports 1 through 8 are marked as 1, receiving ports 9 through 16 are marked as 2, and dummy ports are marked as 0. Note that the dummy ports in lens design are sometimes necessary in order to reduce the side wall reflections as well as to increase the adjacent beam port isolations. In the current lens, all ports are implemented by physical triangular tapered mictorstrip horns, and the transmission lines are built on the same layer using traditional 50-Ω microstrip lines. Port numbers are included in Figure 2 as well to facilitate the analysis in forthcoming sections.

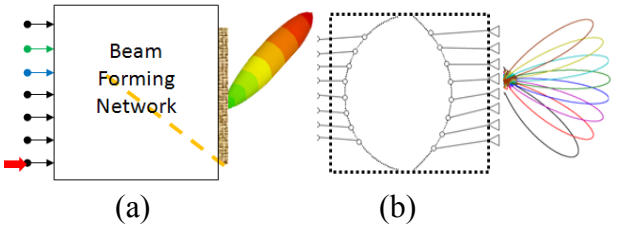

(a) (b)

Fig. 1. Microwave lens as beam forming network.

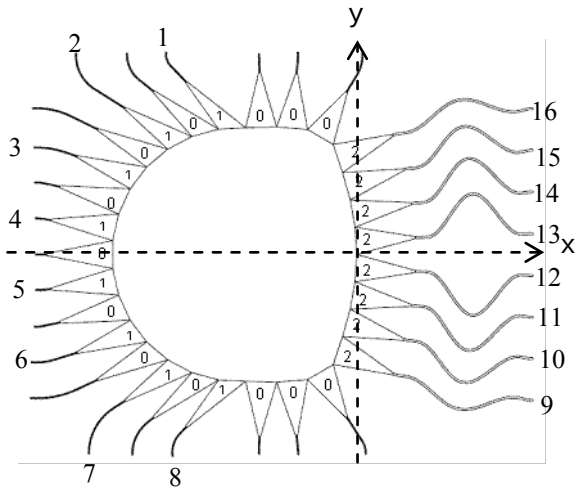

Fig. 2. Rotman lens layout.

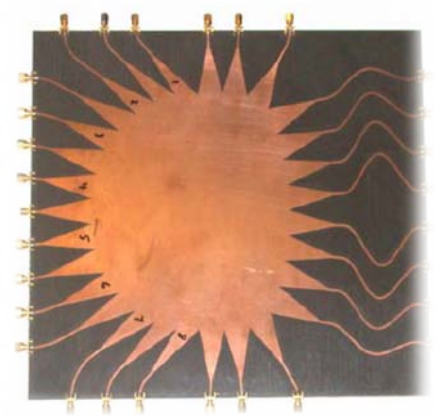

Fig. 3. Fabricated Rotman lens prototype.

Fig. 3 is the Rotman lens prototype that was fabricated by the Army Research Lab in Adelphi, MD. This lens was designed at center frequency 4.6 GHz, and extensive S-parameter measurements were taken [7]. This printed circuit lens is the product of a series of Rotman lens developments that have been going on at ARL for a number of years [8]. The results in [7] are used in this paper for validating the FEKO model as well as evaluating the lens performance. Some technical parameters used to construct the lens are listed in Table 1.

Table 1. Rotman lens Parameters.

Symbol	Quantity	Value
f_0	Center Frequency	4.6 GHz
B	Testing Band	4-5 GHz
N_b	Beam Port #	8
N_r	Receive Port #	8
ε_r	Relative Permittivity	2.3
tanδ	Loss tangent	0.0012
σ	Conductivity	5.7 e+7
d	Array Spacing	31.9mm
h	Substrate Thickness	0.508 mm
t	Copper thickness	0.07 mm

*Terminal impedance is 50Ω, so the width of the transmission line is designed approximately 1.526 mm.

III. SIMULATION AND MEASUREMENT RESULTS

In this section, we focus on the full wave simulation in FEKO and its validation versus measurement data. We shall keep in mind that Rotman lens is a multiple-port-network structure. While conducting comparisons, both beam-port to receiving-port coupling, or transmission factor, across frequency and coupling from a beam-port to all receiving aperture ports at single frequency, in both amplitude and phase, are important.

The simulation was based on the Planar Green's Function solver in FEKO by assuming an infinite ground plane. Each input/output is modeled as microstrip port. Each port is assigned 50-Ohm load so that when any beam port is excited, all others are terminated. The S-parameters between the beam ports and the receiving ports are registered. Eleven discrete frequency steps from 4 to 5 GHz were simulated. The entire simulation took 8.965 hours in a 64-bit workstation, using 4-core Intel(R) Xeon(R) 3.0GHz CPUs. The peak memory consumption of all processes was 2.136 GByte.

For performance across the receiving aperture, the amplitude and phase couplings are studied when single ports are excited at a single frequency. For performance across the frequency band, we can study the beam-port to receiving-port couplings in amplitude and phase. Due to the symmetric structure of a Rotman lens, it is not necessary to compare the results for all ports. Typical ports and comparison strategies are listed in Table 2. In this section, we present a comprehensive comparison between FEKO and measurements. Next section focuses on the performance analysis based on the beam-port to receiving-port coupling discussed in this section.

Table 2. Comparison objects between FEKO simulations and measurements.

Uppercase	1. Couplings across aperture at 4.6 GHz				2. Couplings Across 4-5 GHz			
Feed Port	1	2	3	4	5	6	7	8
Receiving Port	9–16	9–16	9–16	9–16	13	14	15	16
Amplitude	√	√	√	√	√	√	√	√
Phase	√	√	√	√	√	√	√	√
Figures	Fig. 5, Fig. 6				Fig. 7, Fig. 8			

1. Couplings Across Aperture at 4.6 GHz

In both simulation and measurements, the data achieved is more or less the single port-to-port S-parameters with amplitude and phase information. For lens design, a primary objective is for the single port excitation to produce the right amplitude taper and linear phase information across the receiving array aperture at the desired frequency, as indicated in Fig. 4.

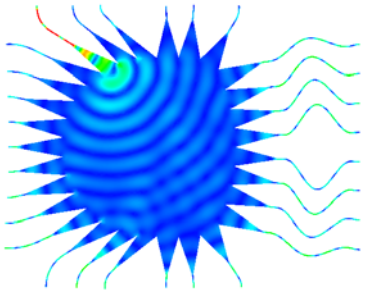

Fig. 4. Surface current for single port excitations.

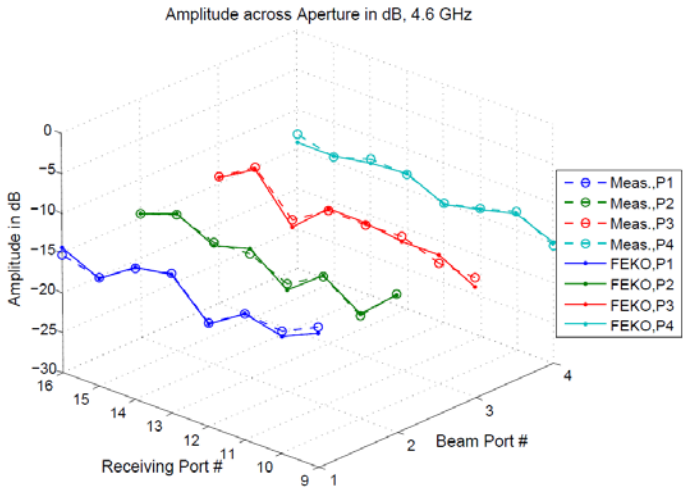

Fig. 5. Comparison between FEKO and measurements for amplitude taper across the aperture at 4.6 GHz.

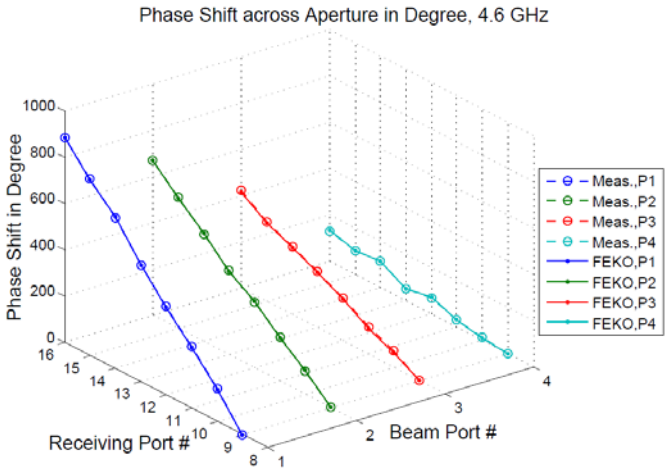

Fig. 6. Comparison between FEKO and measurements, for phase shift across the aperture at 4.6 GHz.

In Fig. 5 and Fig. 6 we arrange the amplitude coupling and phase shift between beam ports (1-4) and all receiving ports (9-16) in 3-D plots. It is observed that the amplitude varies along -15dB for all four port excitations. However, as the beam port moves into the center (from 1 to 4), there is a trend that the amplitude fluctuations saturate. From the phase shift perspective, both simulation and measurements show good agreements and the lens achieves a linear phase shift across the aperture. The phase shift for the large angle beam port (e.g. port 1) has a higher slope than the center port (e.g. port 4). Ideally, the lens is desired to have uniform amplitude taper for highest gain or other amplitude tapers for low sidelobes, and perfect linear phase shift for beam scanning. The errors occurred over the ideal case are considered in the error analysis, which will be explained in the next section.

2. Couplings Across Aperture Across 4-5 GHz

The insertion loss across frequency for single beam-port to receiving-port is another important factor from the communications system design point of view. This reflects how much of gain variation tolerance over the frequency the device possesses. Besides, the phase variations across the frequencies may be significant if the medium is dispersive.

To illustrate the comparison results between FEKO and measurements across 4-5GHz, according to Table 2, we plot the amplitude and phase couplings between the chosen beam ports (5, 6, 7, 8) and chosen receiving ports (13, 14, 15, 16) in Fig. 7 and Fig. 8. It is observable that the simulation agrees well with the measurements. However, it is also noticed that the amplitudes encounter higher attenuation at certain frequencies for different port couplings. This is probably due to two factors: the reflection within the cavity and the different beam port frequency responses.

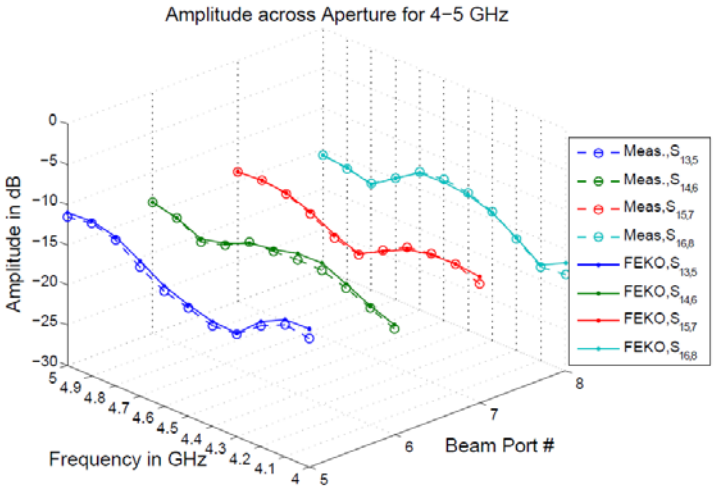

Fig. 7. Port to port amplitude coupling comparison between FEKO and measurements for 4-5 GHz.

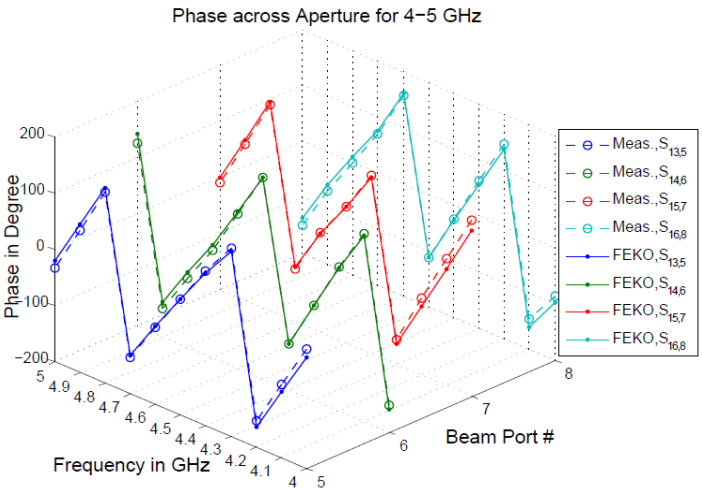

Fig. 8. Port to port phase coupling comparison between FEKO and measurements for 4-5 GHz.

IV. PERFORMANCE ANALYSIS

So far we have been able to do accurate comparison between FEKO and measurement, but we have not interpreted the results in a way to assist the lens optimizations. To conduct lens optimization, it is necessary to know how much the results deviate from the objectives. Although the goal of this section is not to conduct lens optimization, it helps to focus on the error analysis for general lens designs from the perspectives of phase, amplitude and pattern, which are essential components of lens optimization. In the next section, we discuss some of the full wave lens optimization strategies.

The general objective of the lens design assumes to achieve uniform amplitude tapering so as to yield maximum gain, and perfect linear phase shift across the aperture so as to produce stable beams. Resulting from both factors, the true time delay is also a key objective of lens design, meaning, the scanning pointing direction should not change as the frequency varies. In this section, we analyze the amplitude, phase and the scanning direction errors.

1. Amplitude error analysis

In Fig. 5 we showed the amplitude taper across the aperture for different beam port excitations. For each beam port, there are corresponding amplitude errors. Fig. 9 shows the amplitude errors across the aperture for beam port 4 at 4.6 GHz. The standard deviation among all ports can also be used to assess the variation of the amplitude errors. Fig. 10 illustrates standard deviations across the receiving ports for all beam ports at 4.6GHz. It is noted that the deviation from uniform amplitudes is higher at edge beam ports relative to the center beam ports. This may be due to the more symmetric view of the receiving ports for the center beam ports.

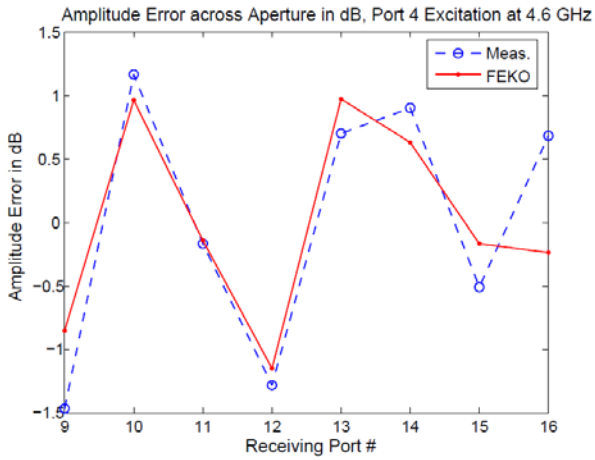

Fig. 9. Amplitude errors across the output ports for port 4 excitations at 4.6GHz.

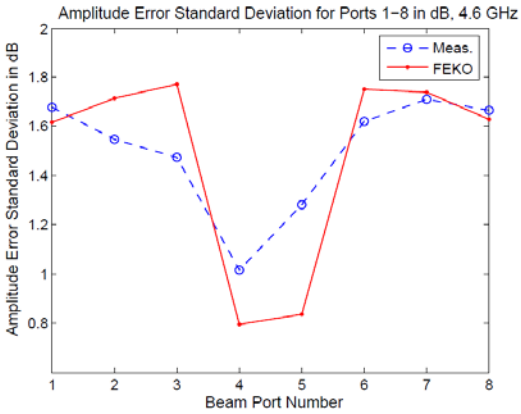

Fig. 10. Amplitude error standard deviation for all beam ports across aperture at 4.6GHz.

Fig. 11 plots the amplitude deviations for all beam ports at various frequencies. It is found that the lens under test maintains average amplitude error of about 1.5dB for all beam ports across the entire frequency band of interest. As the frequency increases, both measurement and FEKO indicate that the amplitude variation increases.

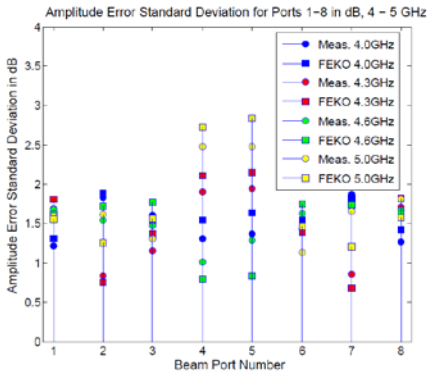

Fig. 11. Amplitude error standard deviation for all beam ports across aperture at 4-5GHz.

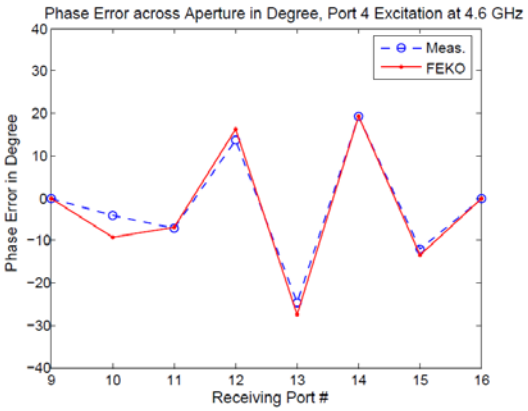

Fig. 12. Phase errors across the output ports for port 4 excitations at 4.6GHz.

2. Phase Error Analysis

The phase shift representation at single frequency was shown in Fig. 6. The phase error occurs when phase shift is not linear with the receive element location. Similar to amplitude errors, phase errors across aperture are different for different beam ports. Example for port 4 excitation at 4.6 GHz is shown in Fig. 12. The phase error standard deviations for all beam ports at 4.6 GHz are shown in Fig. 13. Note that the center beam ports 4 and 5 have exhibited high phase errors up to 15 degrees for the given lens. This may be due to the fact that the lens design and the transmission line length were optimized to produce two perfect focal points off axis in the tri-focal lens design.

Fig. 14 plots the phase error deviations for all beam ports at 4-5 GHz. It is found that the lens under test has average phase error of about 12 degrees for all beam ports across the entire frequency band of interest. As the frequency increases, the variations in phases increase as well, indicating that more attention should be paid to the high frequency operation during the initial formulation.

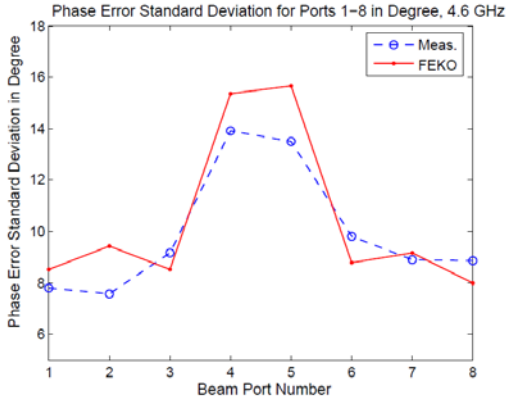

Fig. 13. Phase error standard deviation for all beam ports across aperture at 4.6GHz.

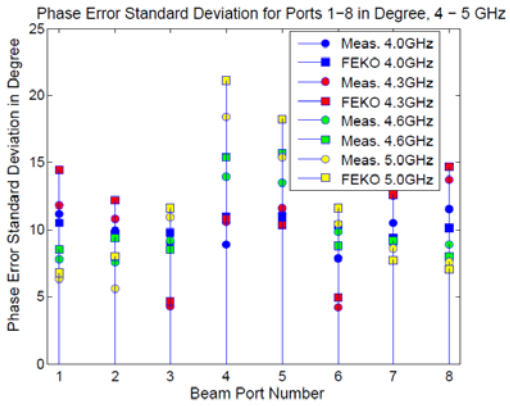

Fig. 14. Phase error standard deviation for all beam ports across aperture at 4.6GHz.

3. Array Factor Analysis

Whether the amplitude variations in Fig 11 and the phase variations in Fig. 14 are acceptable or not depends on the resulting array performance. Typically, amplitudes and phases affect side lobe levels, and the scanning directions. These parameters can be estimated by calculating the array factors, in other words, solving the pattern for isotropic radiation elements.

We investigate the pattern performance by calculating the array factor at the lowest frequency, 4GHz, and the highest frequency, 5GHz. The following plots assume a linear array with uniform spacing of 31.9mm. Both measurement and simulation data are used in Fig.

15 and Fig. 16 for 4 GHz and 5 GHz, respectively. For single frequency operation, the lens scans up to ±45° in eight discrete steps, which result from the eight beam port excitations. In general, as the scanning angle increases, gain decreases and the beam width increases. Comparison between Fig. 15 and Fig. 16 indicates that the beam width decreases and highest gain increases as the frequency increases. Besides, as implied by the high variations in both phase and amplitude tapering at higher frequency, patterns at 5GHz reflect higher gain variations than that at 4GHz.

We also investigate the true time delay behavior for the given Rotman lens. As it shows in Fig. 17, the scanning angle variations between 4GHz and 5GHz change between 0.54° and 1.45°. The beam pointing directions have slightly higher errors at the high scan angles. Note that both measurement and FEKO have predicted asymmetric patterns between 1-4 port excitations and 5-8 port excitations due to possible implementation errors.

In the error analysis presented in this, we processed the phase errors in terms of linear phase shift, calculated amplitude errors based on uniform tapering objectives and estimated the pattern performance based on true time delay property. FEKO simulation and measurements have demonstrated consistent results. The fabricated lens can be characterized by average amplitude errors of 1.5 dB, phase errors of 12 degrees, true time delay with tolerance of less than 1.5 degrees across 4-5 GHz.

There are several strategies for improving the microwave lens design using the full wave analysis. The next section will address some of these strategies.

IV. DISCUSSION ON PERFORMANCE IMPROVEMENTS

In previous sections, we have shown that the amplitude and phase errors can be accurately estimated by measurements and full wave simulations. The former is considered a sure validation, while the latter is a fast way to conduct lens optimizations. The amplitude errors may be caused by the unbalanced propagation directions as well as the reflections within the cavity. The phase errors are caused by the phase center shift as well as the reflections within the cavity. We list several possibilities of improvement below.

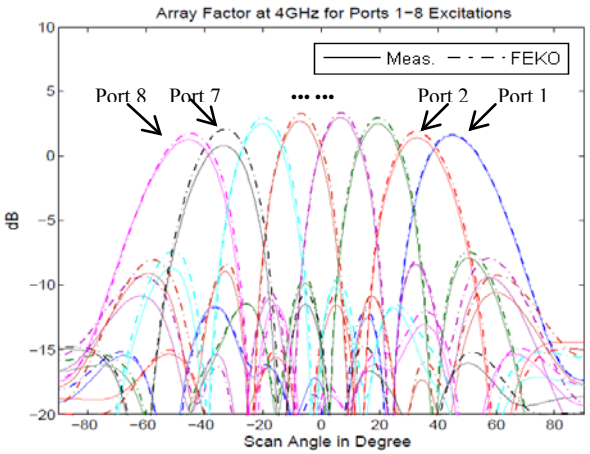

Fig. 15. Array factor for all beam port excitations at 4GHz based on measurement and simulation.

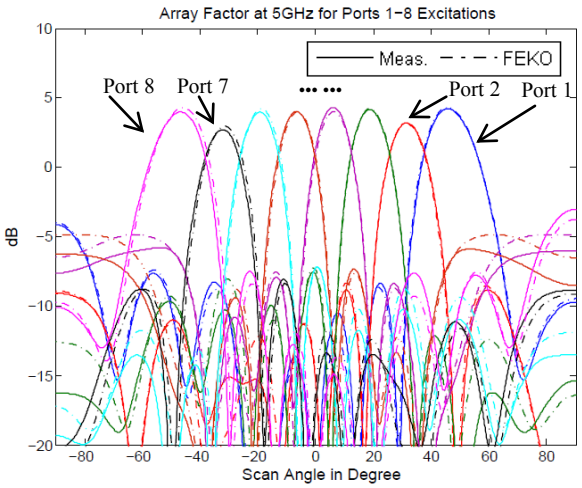

Fig. 16. Array factor for all beam port excitations at 5GHz based on measurement and simulation.

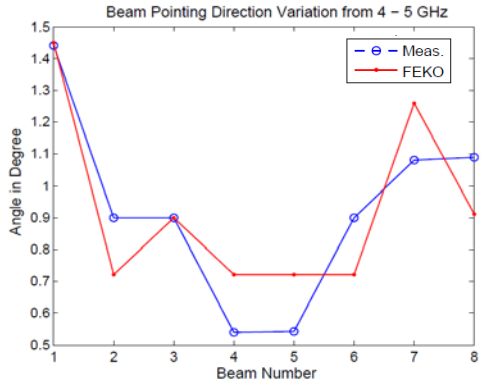

Fig. 17. Scanning angle variation between 4GHz and 5GHz.

1. Beam Port Pointing Direction

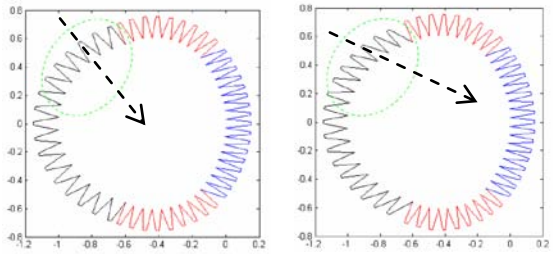

Fig. 18. Beam Port Porting Direction Layout.

The beam port pointing direction, shown in Fig. 18, affects the gain pattern of each port excitation. Typical lenses are designed with the beam ports pointing to the origin of the structure or the center of the receiving ports. However, different subtended angles caused by different pointing angles may yield the desired amplitude distributions along the aperture.

2. Sidewall Freedom of Designs

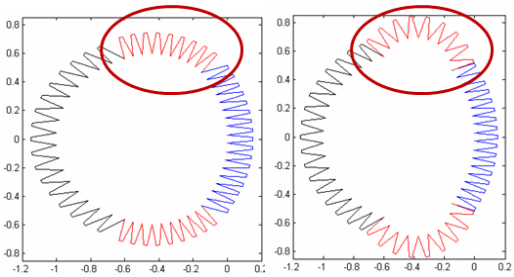

Fig. 19. Lens layout with different sidewalls.

As it shows in [9], the sidewall dummy port terminations play important rule in reducing the reflections in the cavities. To maximize the absorbing ratio or minimize the reflection in certain directions, the sidewall curvature (Fig. 19), as well as the port sizes are essential parameters. The parametric studies of sidewall optimization have not been reported by full wave analysis so far.

3. Tapered Horn Optimization

When a single beam port is excited, all dummy ports and other beam ports are loaded in matched terminations. The geometry of the tapered printed feed elements greatly affects their reflection coefficients. It also affects the operational bandwidth of the lens. So far, most printed Rotman lenses have adopted triangular shape taper horn due to its simplicity. However, it has been found that such tapered line is not optimized, hence has high return loss. Several alternative tapered horns as it indicates in Figure 20 are worth investigating for the optimal frequency response.

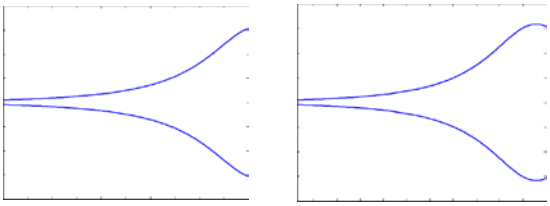

Fig. 20. Tapered horn with different geometries.

Using full wave simulation to optimize lens design has not been extensively addressed. There are more design freedoms than the ones listed above to improve its performance, such as phase center variations versus frequency and mismatch between the cavity and the tapered port junctions, etc. The evolving efficient full wave simulators will soon lead to designs of low amplitude errors, low phase errors, and wideband microwave lenses.

V. CONCLUSION

In this paper we investigated Rotman lens' amplitude, phase and pattern performance by using measurements and full wave simulations. We demonstrated that FEKO is accurate to estimate such parameters based on measurement validations of a given prototype lens. Analysis results show that this lens has average amplitude error of 1.5dB, phase error of 12 degrees, and true time delay tolerance angle of 1.5 degrees across a frequency band 4-5GHz. The presented lens is not optimized, but a few improvement strategies by using full wave simulations are proposed.

REFERENCES

[1] W. Rotman and R. Turner, "Wide-angle Microwave Lens for Line Source Applications," *IEEE Transactions on Antennas and Propagation*, vol. 11, pp. 623-632, 1963.

[2] C. Rappaport and A.I. Zaghloul, "Optimized Three-dimensional Lenses for Wide-angle Scanning," *IEEE Transactions on Antennas*

and Propagation, vol. 33, pp. 1227-1236, 1985.

[3] J. Dong, A. I. Zaghloul, and R. Rotman, "Non-Focal Minimum-Phase-Error Planar Rotman Lens," in URSI National Radio Science Meeting, Colorado, 2008.

[4] C. W. Penney, R. J. Luebbers, and E. Lenzing, "Broad Band Rotman Lens Simulations in FDTD," in IEEE Antennas and Propagation Society International Symposium, 2005.

[5] J. Silvestro, M. Longtin, S. Din-Kow, and Z. Cendes, "Rotman Lens Simulation using the Finite Element Domain Decomposition Method," in IEEE Antennas and Propagation Society International Symposium, 2005.

[6] J. Dong, A.I. Zaghloul, and R. Rotman, "A Fast Ray Tracing Method for Microstrip Rotman Lens Analysis," in XXIXth URSI General Assembly Chicago, 2008.

[7] S. Weiss, S. Keller, and C. Ly, "Development of Simple Affordable Beamformers for Army Platforms," in Proceedings of GOMACTech-07 Conference Lake Buena Vista, FL, 2006.

[8] O. Kilic and R. Dahlstrom, "Rotman Lens Beam Formers for Army Multifunction RF Antenna Applications," in IEEE Antennas and Propagation Society International Symposium, 2005.

[9] J. Dong, Hsu-Cheng Ou, A. I. Zaghloul, "Measurement Investigation of Microstrip Lens Sidewall's Termination", USNC/URSI National Radio Science Meeting, South Carolina, June 2009.

Junwei Dong was born in Hebei, China, in 1983. He received B.S. degree in Measurement & Control and Instrumentation (Signal Processing) from Jilin University, Jilin, China, in 2006. He received his M.S. and Ph.D. in Electrical Engineering at Virginia Polytechnic Institute and State University (Virginia Tech), Virginia, USA, in 2009.

He joined the Virginia Tech Antenna Group (VTAG) as a graduate student in 2006, where he conducted research on antennas, microwave lens designs and electromagnetic simulations. After graduation, he joined Microwave Engineering Corporation (MEC), North Andover, MA as a research scientist. He currently conducts research on microwave component optimization and fabrication techniques.

Amir I. Zaghloul is with the US Army Research Lab (ARL) on an IPA (Inter-Governmental Personnel Act) agreement with Virginia Polytechnic Institute and State University (Virginia Tech), which he had joined in 2001 as Professor in the Bradley Department of Electrical and Computer Engineering. Prior to Virginia Tech, he was at COMSAT Laboratories for 24 years performing and directing R&D efforts on satellite communications and antennas. He is a Fellow of the IEEE, an Associate Fellow of The American Institute of Aeronautics and Astronautics (AIAA), a Member of Commissions A, B & C of the International Union of Radio Science (URSI), and a member of the Board of the Applied Computational Electromagnetics Society (ACES). He was the general chair of the 2005 "IEEE International Symposium on Antennas and Propagation and USNC/URSI Meeting," held in Washington, D.C.

Dr. Zaghloul received the Ph.D. and M.A.Sc. degrees from the University of Waterloo, Canada in 1973 and 1970, respectively, and the B.Sc. degree (Honors) from Cairo University, Egypt in 1965, all in electrical engineering.

Rensheng Sun was born in Heilongjiang, China, in 1975. He received the B.E. degree from Tsinghua University, Beijing, China, in 1999, the M.S. degree from Villanova University, Villanova, PA, in 2002, and Ph.D. degree from Michigan State University, East Lansing, MI, in 2005, all in electrical engineering.

He served as a Visiting Assistant Professor in the Department of Electrical and Computer Engineering at Michigan State University during Fall Semester, 2005. Since January 2006, he has been working as a Senior Application Engineer at

EM Software & Systems (USA) Inc., Hampton, VA. His research interests include computational electromagnetics, antenna design, and multiphysics modeling. He is a member of IEEE, AMTA, Eta Kappa Nu, and Tau Beta Pi.

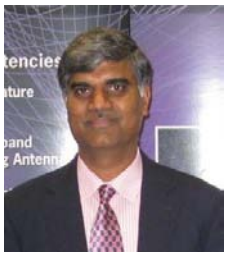

C. J. Reddy received B.Tech. degree in Electronics and Communications Engineering from Regional Engineering College (now National Institute of Technology), Warangal, India in 1983. He received his M.Tech. degree in Microwave and Optical Communication Engineering and Ph.D. degree in Electrical Engineering, both from Indian Institute of Technology, Kharagpur, India, in 1986 and 1988 respectively. From 1987 to 1991, he worked as a Scientific Officer at SAMEER (India) and participated in radar system design and development. In 1991, he was awarded NSERC Visiting Fellowship to conduct research at Communications Research Center, Ottawa, Canada. Later in 1993, he was awarded a National Research Council (USA)'s Research Associateship to conduct research in computational electromagnetics at NASA Langley Research Center, Hampton, Virginia. Dr. Reddy worked as a Research Professor at Hampton University from 1995 to 2000, while conducting research at NASA Langley Research Center. During this time, he developed various FEM codes for electromagnetics. He also worked on design and simulation of antennas for automobiles and aircraft structures. Particularly development of his hybrid Finite Element Method/Method of Moments/Geometrical Theory of Diffraction code for cavity backed aperture antenna analysis received Certificate of Recognition from NASA.

Currently, Dr. Reddy is the President and Chief Technical Officer of Applied EM Inc, a small company specializing in computational electromagnetics, antenna design and development. At Applied EM, Dr. Reddy successfully led many Small Business Innovative Research (SBIR) projects from the US Department of Defense (DoD). Some of the technologies developed under these projects are being considered for transition to the DoD. Dr. Reddy also serves as the President of EM Software & Systems (USA) Inc. At EMSS (USA), he is leading the marketing and support of commercial 3D electromagnetic software, FEKO in the US, Canada, Mexico and Central America.

Dr. Reddy is a Senior Member of the IEEE. He is also a member of Applied Computational Electromagetic Society (ACES) and serves as a member of Board of Directors. He has published more than 60 referred journal articles and conference papers.

Steven J. Weiss was born in Utica, NY in 1955. He graduated from The George Washington University in 1995 with a doctoral degree in Electrical Engineering. He is presently with the Army Research Lab working with antenna systems. His research areas include specialized antennas for military applications. He is a Senior Member of the IEEE Antennas and Propagation Society.